TECHNICAL REPORT

ISO/TR 12112

First edition

Actallic materials — Principles and designs for multiaxial fatigue testing Matériaux métalliques — Principes et conceptions associés aux essais de fatigue multiaxiale Ether of the conception of the conception





© ISO 2018

All rights reserved. Unless otherwise specified, or required in the context of its implementation, no part of this publication may be reproduced or utilized otherwise in any form or by any means, electronic or mechanical, including photocopying, or posting on the internet or an intranet, without prior written permission. Permission can be requested from either ISO at the address below or ISO's member body in the country of the requester.

ISO copyright office CP 401 • Ch. de Blandonnet 8 CH-1214 Vernier, Geneva Phone: +41 22 749 01 11 Fax: +41 22 749 09 47 Email: copyright@iso.org

Website: www.iso.org Published in Switzerland

Co	ntent	S	Page
For	eword		v
Intr	oductio	n	vi
1	Scon	e	1
2	-	native references	
3	Term	is and definitions	1
4		eral principles.	2
	4.1	Methodology	2
	4.2	Historical development	
	4.3	Specific multiaxial test methods	6
		4.3.1 Bending + torsion[6] 4.3.2 Axial + torsion[7]	6
			6
		4.2.4 Avial Lintarnal Laytarnal programs[9]	6
		435 Axial + internal + external pressure + torsion[10]	6
		4.3.6 Cruciform — LCF[11]	6
		4.3.7 Cruciform — Crack growth[12]	7
	4.4	Multiaxial fatigue analysis	7
		4.4.1 Computer aided design	7
		4.4.2 Fatigue life prediction	7
	4.5	4.3.5 Axial + internal + external pressure + torsion[10] 4.3.6 Cruciform — LCF[11] 4.3.7 Cruciform — Crack growth[12] Multiaxial fatigue analysis 4.4.1 Computer aided design 4.4.2 Fatigue life prediction Multiaxial fatigue failure criteria	8
5	Avial	L tarrian tarting systems and enacimen decign	Q
3	5.1	Historical development Specimen design 5.2.1 Design considerations	9
	5.2	Specimen design	11
		5.2.1 Design considerations	11
		5.2.2 Design recommendations	11
		5.2.3 Comparison with ASTM E2207[4]	11
	5.3	Machine design	
		5.3.1 Frame	
		5.3.2 Loadcells	
		5.3.3 Strain measurement	
		5.3.4 Control	
		5.3.5 Data acquisition	
		5.3.6 Software	
6		iform testing systems and specimen design	
	6.1	Historical development	
	6.2	Specimen design	
	6.3	Machine design	
	XX	6.3.1 Frame	
	S.	6.3.2 Loadcells 6.3.3 Strain measurement	
		6.3.3 Strain measurement	
		6.3.5 Control	
		6.3.6 Data acquisition	
		6.3.7 Software	
7	A 1		
7		l + differential pressure systems and specimen design	10
	7.1 7.2	Historical development Specimen design	
	1.4	7.2.1 Design considerations	
		7.2.2 Design recommendations	
		7.2.3 Axial stress due to pressure	
	7.3	Machine design	
		7.3.1 Frame	

ISO/TR 12112:2018(E)

7.3.2 7.3.3 7.3.4 7.3.5 7.3.6 7.3.7 7.3.8 7.3.9	Pressure containment Differential pressure Force measurement Pressure measurement Strain measurement Control Data acquisition Software	20 20 20 20 20 20 20 20
Annex A Historical a	analysis of specimen geometry	22
STANIC	analysis of specimen geometry Citck to view the full profit of the state of the st	REOTRAZA ZA AZA ZA

iv

Foreword

ISO (the International Organization for Standardization) is a worldwide federation of national standards bodies (ISO member bodies). The work of preparing International Standards is normally carried out through ISO technical committees. Each member body interested in a subject for which a technical committee has been established has the right to be represented on that committee. International organizations, governmental and non-governmental, in liaison with ISO, also take part in the work. ISO collaborates closely with the International Electrotechnical Commission (IEC) on all matters of electrotechnical standardization.

The procedures used to develop this document and those intended for its further maintenance are described in the ISO/IEC Directives, Part 1. In particular the different approval criteria needed for the different types of ISO documents should be noted. This document was drafted in accordance with the editorial rules of the ISO/IEC Directives, Part 2 (see www.iso.org/directives).

Attention is drawn to the possibility that some of the elements of this document may be the subject of patent rights. ISO shall not be held responsible for identifying any or all such patent rights. Details of any patent rights identified during the development of the document will be in the Introduction and/or on the ISO list of patent declarations received (see www.iso.org/patents)

Any trade name used in this document is information given for the convenience of users and does not constitute an endorsement.

For an explanation on the voluntary nature of standards, the meaning of ISO specific terms and expressions related to conformity assessment, as well as information about ISO's adherence to the World Trade Organization (WTO) principles in the Technical Barriers to Trade (TBT) see the following URL: www.iso.org/iso/foreword.html.

This document was prepared by Technical Gammittee ISO/TC 164, Mechanical testing of metals, Subcommittee SC 4, Fatigue, fracture and toughness testing.

© ISO 2018 – All rights reserved

Introduction

Structural components in industry are frequently subject to some form of multiaxial stressing. Fatigue cracks generally initiate from surface defects or discontinuities and are thus primarily influenced by the surface biaxial stress system. This can vary from equibiaxial, where surface principal stresses are equal in magnitude and sign (present under conditions of pressurization, rotation and thermal loading) to pure shear where surface stresses are equal in magnitude, opposite in sign (as in shafts and shear panels).

The majority of fatigue test data gathered worldwide have been and will continue to be under uniaxial conditions for reasons of simplicity and cost. A secondary goal of multiaxial testing is therefore to develop behavioural models which relate failure under specified multiaxial conditions to established uniaxial cases.

standards is o conf. circly to view the full part of isolars. This document utilizes data gathered from the past 80 years spanning most multiaxial fatigue research. It can be of interest to new researchers in the field and form a basis for full International Standards as the need arises.

Metallic materials — Principles and designs for multiaxial fatigue testing

Scope

This document discusses the general principles of multiaxial fatigue testing and the design recommendations for specific classes of multiaxial testing machines and test specimens. TR 12/12:25

2 **Normative references**

There are no normative references in this document.

Terms and definitions

For the purposes of this document, the following terms and definitions apply.

ISO and IEC maintain terminological databases for use in standardization at the following addresses:

- ISO Online browsing platform: available at https://www.iso.org/obp
- IEC Electropedia: available at http://www.electropedia.org/

3.1

biaxial strain ratio

ratio of the surface principal strains, smaller/larger

3.2

biaxial stress ratio

ratio of the surface principal stresses, smaller/larger

principal strains

 $\varepsilon_1 > \varepsilon_2 > \varepsilon_3$

principal direct strains at a point in a multiaxial strain field

3.4

principal stresses

 $\sigma_1 > \sigma_2 > \sigma_3$

principal direct stresses at a point in a multiaxial strain field

Poisson's ratio

negative ratio of transverse to longitudinal strain under uniaxial tensile stressing

3.6

specimen diameter

diameter of a cylindrical tubular specimen

Note 1 to entry: The symbols d_0 , d_i and d_m are used to express outside, inside and mean diameters, respectively.

ISO/TR 12112:2018(E)

3.7

parallel length

parallel length of a cylindrical tubular specimen

3.8

fillet radius

fillet radius of a cylindrical tubular specimen

3.9

directional suffix

suffix identifying a direction in a cylindrical tubular specimen

Note 1 to entry: The suffixes z, r and θ are used to express axial, radial and circumferential directions, respectively.

3.10

strain component suffix

suffix identifying a strain component

Note 1 to entry: The suffixes e, p and t are used for elastic, plastic and total strain components, respectively.

3.11

internal pressure

internal pressure within a cylindrical tubular specimen

General principles

4.1 Methodology

to view the full PDF Multi-axial fatigue testing sets out to simulate the dynamic stress-strain conditions at key locations on components, on test specimens of constant geometry for a given test series, and to determine the cyclic stress-strain history, crack initiation and propagation behaviour, fatigue life and failure mode.

Dependent on the level of geometric constraint in the real component, it can be more useful to test specimens under stress or strain control, e.g. a test specimen representative of a relatively unconstrained gas turbine blade can be tested in stress control whereas it can be more relevant to utilize strain control for a test specimen simulating part of a steam turbine disc subject to thermal straining during start-up.

Further, where stress amplitudes are sufficient to take test specimen materials well into the region of cyclic plasticity (CF), it can be preferable to employ strain control in order to better control cyclic amplitude during the test and failure at end of test.

Historical development

Multiaxial fatigue has been addressed since the 1930s. Initially, testing machine and specimen designs were created to address specific biaxial stress conditions, e.g. torsion, bending + torsion, cantilever bending, anticlastic bending and plate pressurization. However, a criticism of much of the early research was that specimen design had to change in order to change the biaxial stress or strain ratio, leading to uncertainty in the interpretation of results.

The benefit of being able to test a single specimen design over a wide range of biaxiality led to the choice of two generic specimen types, tubular and cruciform, together with associated multi-axis testing machine designs.

Table 1[5] summarizes the attributes of the different test methods applicable to tubular and plate specimens.

Biaxiality is shown in terms of the range of surface strains with ε_1 held constant. Only cruciforms and systems employing axial force plus internal and external pressure are capable of applying fully reversed fatigue cycles over the full range of biaxiality ($-1 \le \phi \le +1$) to test specimens.

Buckling is a key concern in the design of effective LCF specimens.

A reasonable gauge area of essentially constant strain is beneficial.

Ideally, strain should be constant through the thickness.

If all the applied forces are carried by the gauge area, then all stresses and strains can be determined; otherwise, only total (not plastic) strains can be measured.

The ability to visually observe the specimen is useful especially for surface crack monitoring.

Some designs are suitable for high temperature and thermo-mechanical fatigue (TMF) testing.

Systems involving torsion cause the principal axes to rotate up to 45°.

System cost can be scaled by the number of actuators, and therefore closed servo-loops, in the design.

Click to riem the full public closed servo-loops, in the design.

Table 1 — Multiaxial test methods for tubular and plate specimens

No. of actuators propor- tional to cost	1	2	2	2	4
Rota- tion of principal stresses	<u> </u> ^	>			<i>></i>
TMF		>			
High temperature		>	>	<i>></i>	
Grack growth studies		>			\$
Speci- men ob- servation	Ŷ	>	>	65	III POF
Monitoring biaxial σ and ε _P		>	>	ienthei	A
Min. E-gra- dient through	Y	>	Clickto	7	<i>></i>
Invariant σ and ε on gauge area		COM	>	<i>></i>	<i>></i>
Immune to buck- ling	ARDS				
Single geometry	> 	>	>	>	>
Range of surface principal strains	¹ 3	3 ²			
Biaxial specimen schemat- ics and modes of loading					
	Bending + torsion	Axial + torsion	Axial + P _{int}	Axial + Pint + con- stant + Pext	Axial + Pint + Pext + torsion

propor-tional to actuators No. of cost 4 principal stresses tion of Rota-0150/R12112018 studies TMF > High temperature capability > growth studies Crack > Click to view the full PDF servation Speci-men obbiaxial σ Moni-toring and Ep > through thickness dient e-gra-> Invariant on gauge σ and ε > > Immune to buckling Single geome-Range of principal surface strains ω specimen schemat-modes of loading ics and Biaxial **A** Anticlas-tic bend pressuriform LCF ver bend Cantilegrowth zation Cruci-Cruci-Plate form crack

Table 1 (continued)

4.3 Specific multiaxial test methods

4.3.1 Bending + torsion[6]

This was the first technique used to apply combined stresses in high cycle fatigue (HCF) at room temperature. Oscillating vertical forces were applied to a horizontally clamped cylindrical specimen which could be rotated by up to 90° in the horizontal plane so as to introduce bending, bending + torsion, or torsion in the waisted centre section. Specimens were either solid or hollow. A number of these electro-mechanical testing machines were built between 1930 and 1950 to investigate fatigue of aero-engine steels, especially for crankshaft applications.

4.3.2 Axial + torsion[7]

This popular technique employs a single tubular specimen design with a gauge length over which stress and strain are substantially invariant and access for strain measurement and crack monitoring. The principal stress and strain directions progressively rotate through 45° as the test moves from uniaxial to torsion. Elevated temperature testing and thermo-mechanical fatigue (TMF) are achievable with relevant accessories and control software. Despite a limited range of strain biaxiality ($-v \ge \phi \ge -1$), this approach is widespread and standard testing machines with dual servo-hydraulic actuators are available from commercial manufacturers.

4.3.3 Axial + internal pressure[8]

This approach permits a single tubular specimen design with essentially invariant stress and strain over the gauge length. Crack studies are difficult as maximum stress occurs at the bore, so cracks can only be visible after penetration of the wall shortly prior to failure. In addition, cyclic plasticity results in strain ratchetting as external radial compression cannot be applied to fully reverse the stress — strain cycle. Hence this approach is essentially restricted to elastic HCF studies. The testing machine typically utilizes a dual actuator servo-hydraulic design.

4.3.4 Axial + internal + external pressure[9]

This design enables fully reversed cycling without ratchetting because radial compression can be applied. Axial and circumferential stresses and strains are measurable, enabling LCF hysteresis loops on both surface axes, which makes the approach suitable for fundamental behavioural studies. Because a pressure vessel is located around the specimen, visual observations are difficult. Also elevated temperature testing above about 200 °C requires gas pressurization which presents safety issues. By employing variable internal pressure and fixed external pressure, a design with just 2 servo-hydraulic actuators is achievable.

4.3.5 Axial + internal + external pressure + torsion[10]

The addition of torsion introduces rotation of principal stress or strain axes which allows, in principle, material anisotropy and the effects of the different symmetries (in the axial and circumferential directions) to be investigated. The mechanical design is complex with 4 servo-hydraulic actuators, but has been successfully achieved.

NOTE Multiaxial testing machines featuring axial force and differential pressure are typically used for academic research or specific R&D applications, and are usually designed and manufactured to order.

4.3.6 **Cruciform** — **LCF**[11]

Four orthogonal loading arms apply biaxial strain to a central circular gauge area on the specimen. This area is usually spherically recessed on both sides in order to resist buckling and ensure that cracks initiate near the centre. In consequence, the gauge area does not support all the applied forces, i.e. some of the force is shunted around the outside. As a result, stresses and plastic strains are not readily

determinable. However, visual observation of developing fatigue cracks is straightforward and elevated temperature testing, including TMF, is readily achievable.

4.3.7 Cruciform — Crack growth[12]

The four orthogonal arms are slotted to minimize grip constraint. A central square, constant thickness, gauge area typically features a central hole stress raiser to initiate fatigue cracks. There is a large region of essentially constant biaxial strain ideal for crack initiation and propagation studies. Elevated temperature testing, including TMF, is achievable. Maximum compressive strains are limited to avoid buckling in the gauge area and arms.

NOTE Cruciform designs provide the opportunity for testing single geometry plate specimens with dual symmetry over the range of surface biaxiality. Testing systems employ 4 servo-hydraulic actuators within an annular frame and are typically specified according to application and manufactured to order.

4.4 Multiaxial fatigue analysis

4.4.1 Computer aided design

In the design of structural components subject to multiaxial fatigue, it is common to use finite element analysis (FEA) to determine stresses and strains. For elastic behaviour, such analyses are useful to predict stress concentrations and local yield in order to evolve specimen designs.

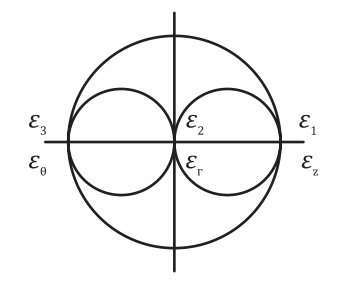
4.4.2 Fatigue life prediction

Yield criteria such as Tresca (maximum shear), Von Mises or octahedral shear strain, coupled with the Palmgren-Miner linear damage hypothesis, are frequently employed to predict "multiaxial fatigue life". However, research evidence does not necessarily support this approach.

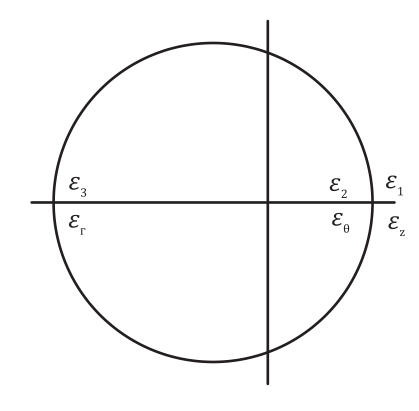
Multiaxial LCF fatigue studies [13][14] on specimens capable of being tested over the full biaxial range showed that Tresca and Von Mises did not correlate all the fatigue life data, especially over the range between uniaxial and torsion, i.e. $(0 \ge b \ge -1)$ and $(-v \ge \phi \ge -1)$.

For example, in Figure 1, Mohr's strain circles drawn with principal strain (ε_1) constant and Poisson's ratio = 0,5, show that the maximum shear strain (γ_{max}) is the lowest in the uniaxial stress ($\phi = -\nu$) case. However, ranking these biaxial fatigue cases from most to least damaging, the order was equibiaxial strain ($\phi = +1$), plane strain ($\phi = 0$), uniaxial stress ($\phi = -\nu$) and pure shear ($\phi = -1$).

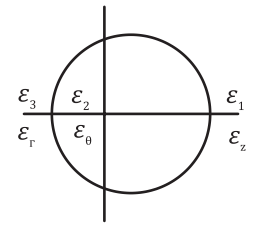
Current consensus 15t indicates that a critical shear plane analysis including, as a modifier, the direct stress or strain acting normal to that plane, offers the best approach to correlating multiaxial fatigue behaviour across the complete range of applied biaxial surface stresses or strains.



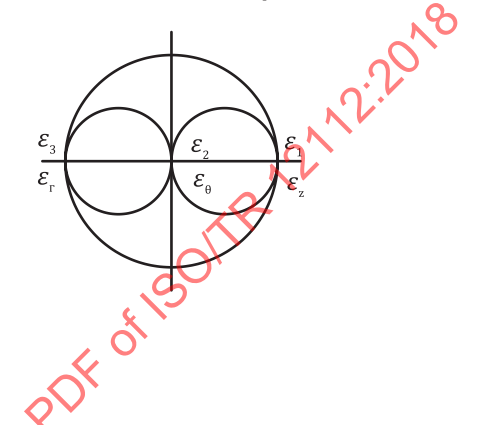
a) Pure shear $(\phi = -1)$



c) Equibiaxial strain ($\phi = +1$)



b) Uniaxial stress ($\phi = -v$)



d) Plane strain (ϕ = 0)

Figure 1 — Mohr's strain circles, ε_1 constant, for Poisson's Ratio (ν) = 0,5

4.5 Multiaxial fatigue failure criteria

The definition of fatigue failure criteria can have a significant effect on attempts to correlate theoretical analysis with experimental results.

Axial force + torsion (without pressurization) results in the gauge area seeing all the applied stresses. The maximum shear strain is always in the surface, except in the uniaxial stress case when there is an equal through-thickness shear strain. Fatigue lives according to stress drop can be readily determined. Stress drop, after any cyclic hardening or softening, is generally considered to be the result of a reduction in load bearing cross sectional area due to cracking.

In the case of cruciform specimens, where actuator forces are partially shunted around the gauge area, a calculated stress drop criterion is sometimes not easy to apply. Fatigue lives are typically determined by the achievement of a specified surface crack length. Through-thickness cracks can still extend in a stable fashion, The relationship between crack length and crack area depends on the biaxial strain ratio.

When internal/external pressurization is used in conjunction with axial force, the gauge area experiences all the applied stresses. However, stress drop is not usually helpful as a failure criterion since, when the crack penetrates the thickness of the specimen (allowing internal and external pressures to interact), the test should be rapidly terminated or unstable rupture can ensue. As a consequence, crack lengths in the surface are relatively short and of different length according to the biaxial strain ratio.

5 Axial + torsion testing systems and specimen design

5.1 Historical development

Axial + torsion enables a single tubular specimen geometry to be tested over a biaxial range $(-\nu \ge \phi \ge -1)$ with convenient access for strain measurement and crack monitoring. Notably, the principal stress and strain directions rotate through 45° as the test moves from uniaxial to torsion.

At Tohoku University, in 1965, data was reported[16] for torsional and uniaxial LCF, derived from separate machines but with identical gauge length geometry, to investigate multiaxial behaviour.

At Kyoto University, the first combined axial + torsional fatigue testing at ambient and elevated temperatures for in-phase and subsequently, in 1968, for out-of-phase cycling [17] was described.

From the 1970s onwards, axial + torsion, closed loop servo-hydraulic, testing machines have been provided by materials testing machine manufacturers and widely used in academia and industrial R&D for HCF, LCF and creep-fatigue testing[18].

TMF using axial + torsion systems has been reported[19] from the 1990s

Figure 2 below depicts an axial + torsion TMF system at the CRIEP (Central Research Institute of Electrical Power Industry) laboratory near Tokyo.

9

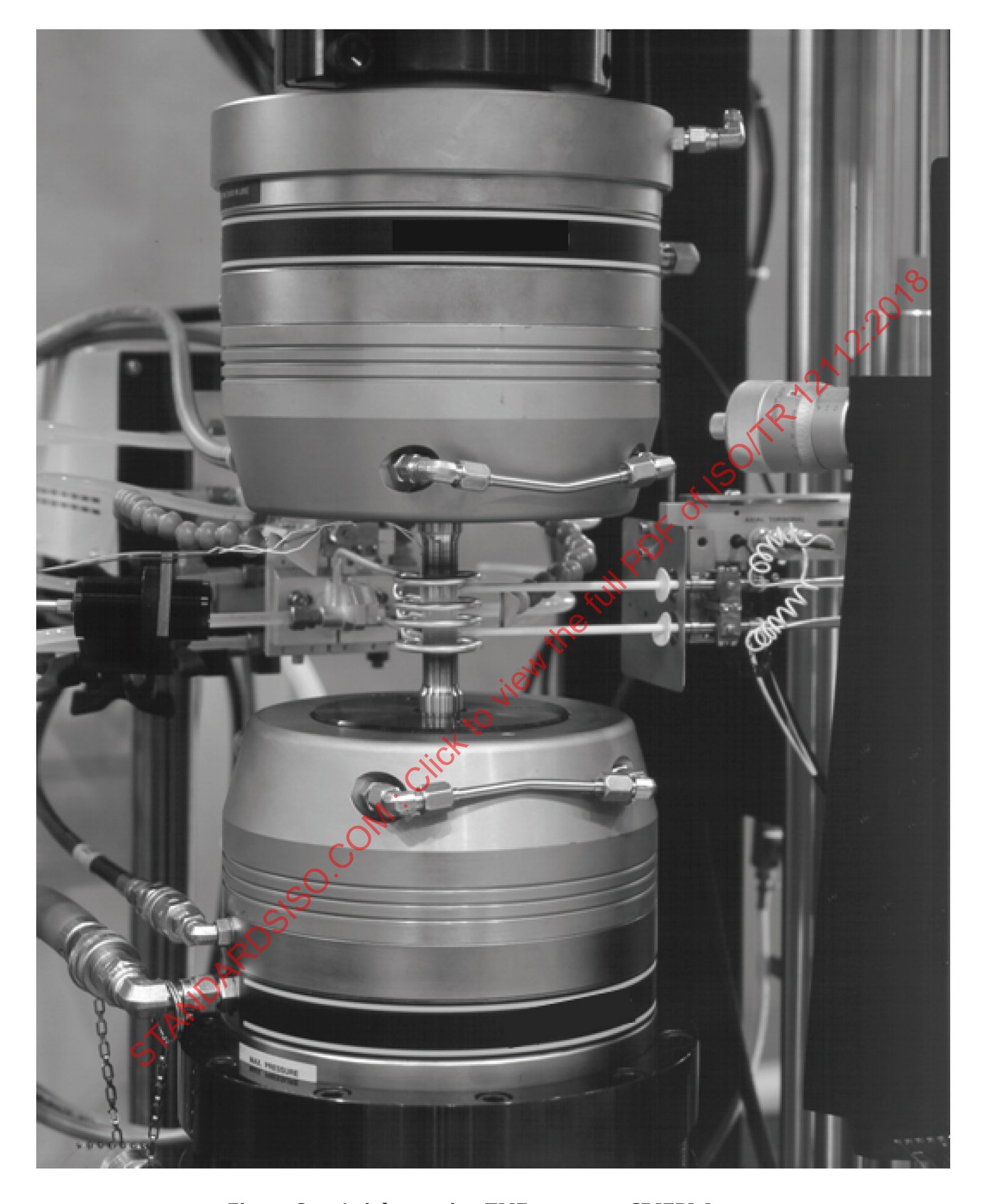


Figure 2 — Axial + torsion TMF system at CRIEPI, Japan

5.2 Specimen design

5.2.1 Design considerations

A single specimen geometry should be maintained for a given test series to validate data intercomparison.

Bending is minimized by ensuring that specimen ends are square to the axis and parallel to each other. It is preferable to locate just one end concentrically, which avoids "S type" bending due to any slight misalignment of the machine grips.

Buckling can occur under axial and torsional conditions. Both elastic and plastic buckling should be considered. Buckling is predominantly influenced by the parallel length (l_p) , mean diameter (d_m) and wall thickness (t) together with (for LCF) the plastic strain range and strain hardening characteristics of the specimen material.

Fatigue strength and life are enhanced by minimizing the stress concentration at the run-out of the fillet radius (*r*) on to the parallel length.

5.2.2 Design recommendations

By considering the geometric ratios $l_{\rm p}/d_{\rm m}$, $r/d_{\rm m}$ and $d_{\rm m}/t$, it is possible to compare the designs of research specimens over the past 50 years. See Annex A, where data has been separately analysed for HCF and LCF.

The ranges for l_p/d_m and r/d_m substantially overlap for LCF and HCF whereas the range for d_m/t is 2 to 3 times lower for LCF, which is significant and reflects plastic buckling resistance.

As a result, recommended ranges for these ratios are indicated below with the lower values providing best resistance to plastic buckling and the higher values best elastic strain uniformity.

$$2 > l_p/d_m > 1$$
 $3 > r/d_m > 1$ $30 > d_m/t > 10$

Figure 3 shows an LCF specimen design with mid value geometric ratios for l_p/d_m and r/d_m and low value ratio for d_m/t .

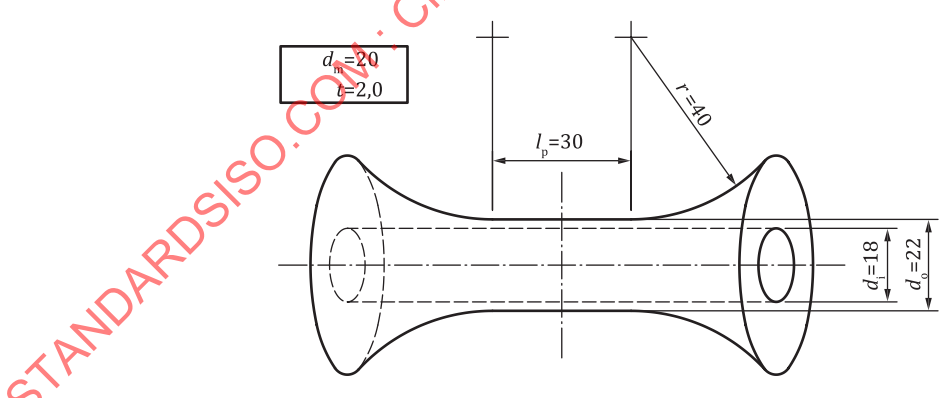


Figure 3 — Axial-torsion LCF fatigue specimen

5.2.3 Comparison with ASTM E2207[4]

ASTM E2207 was first published in 2002 and re-approved in 2008 and 2013¹).

Specimen design is covered in <u>Clause 7</u> and is expressed in terms of geometric ratios to the gauge length outside diameter (d_0).

-

¹⁾ ASTM E2207-08(2013)e1 has been superseded by ASTM E2207-15.

ISO/TR 12112:2018(E)

Annex A includes the ASTM specimen geometry recommendations and their conversion to the form expressed in this document for the indicated typical wall thickness of 2 mm, to enable comparison. Generally the ratios are similar except for fillet radius which is large in relation to the historic mean. Moreover, the ASTM typical specimen is quite large with a billet requirement of circa 50 mm diameter by 230 mm long.

5.3 Machine design

5.3.1 Frame

Axial and torsional stiffness should be maximized to minimize frame deflections. Lateral stiffness should be maximized to minimize axial buckling tendency. Two column frames are typical for LCF and TMF applications. Alignment should be to ISO 23788.

5.3.2 Loadcells

Axial force and torque cells may be individual or combined. Force and torque ratings, stiffnesses and accuracy class 1 to ISO 7500-1 should be specified.

5.3.3 Strain measurement

Extensometers may be separate or integrated. Operating force, clamping force, crosstalk and accuracy class 0,5 to ISO 9513 should be specified. Compatibility with furnaces and environmental chambers should be considered.

5.3.4 Control

Closed loop control should permit bumpless starts and mode transfers between position, force and strain control modes. The control bandwidth should be high enough to accommodate the highest frequency components within the anticipated demand waveforms. Synchronisation of applied waveforms should be better than 0.2° .

5.3.5 Data acquisition

Sampling rate should be sufficiently high to avoid aliasing at the highest anticipated frequency components of measured signals. Data skew between measured signals should be less than 5 μ s.

5.3.6 Software

Results of data analysis should permit independent verification.

6 Cruciform testing systems and specimen design

6.1 Historical development

A specimen design lending itself directly to biaxial testing is a cross-shaped plate, or cruciform, loaded in-plane by four orthogonal actuators.

In the early 1960s, at the Chance Vought Corporation^[20], a rig that was capable of applying biaxial tensile loads to a cruciform specimen was developed.

At Cambridge University^[21], the development of an open loop cruciform testing system based on a stiff octagonal frame carrying four 200 kN double acting actuators was reported in 1967. Further development^[11] to provide full closed loop control was reported in 1975.

In 1985, a new specimen, developed at Sheffield University^[12], was reported featuring a recessed flatbottomed square gauge area connected to the loading arms by sets of fingers (Figure 2). This decoupling geometry enables a substantially uniform strain field ideal for crack growth studies.

Using induction heating, ceramic composite plate samples were tested in a cruciform system at temperatures up to 1800 °C at JUTEM[22] (Japanese Ultra high Temperature Materials Research Centre).

Current research on cruciform systems includes elevated temperature TMF of single crystal super alloys.

6.2 Specimen design

Cruciform specimens are especially suitable for plate materials.

A single specimen geometry should be maintained for a given test series to validate data intercomparison.

The LCF specimen type (see <u>Table 1</u>) is potentially capable of fully reversed elastic-plastic straining over the full range of biaxiality $(+1 \ge \phi \ge -1)$.

Buckling is a significant risk for LCF specimens. Spherical radii are needed on both surfaces to combat it, with smaller radii for higher cyclic plastic strains which reduce the effective size of the central gauge area. A small flat central zone is sometimes introduced to provide a region of relatively uniform strain.

The crack growth specimen (Figure 4), developed at Sheffield University, can be viewed as a quasistandard approach. It features a recessed, flat-bottomed, square gauge area connected to the four loading arms by sets of fingers. This decoupling geometry enables a substantially uniform strain field ideal for crack growth studies.

The crack growth specimen does not permit significant plastic compressive stressing due to buckling of the fingers. This is not a serious problem as crack growth studies are usually carried out in tension-tension stress fields.

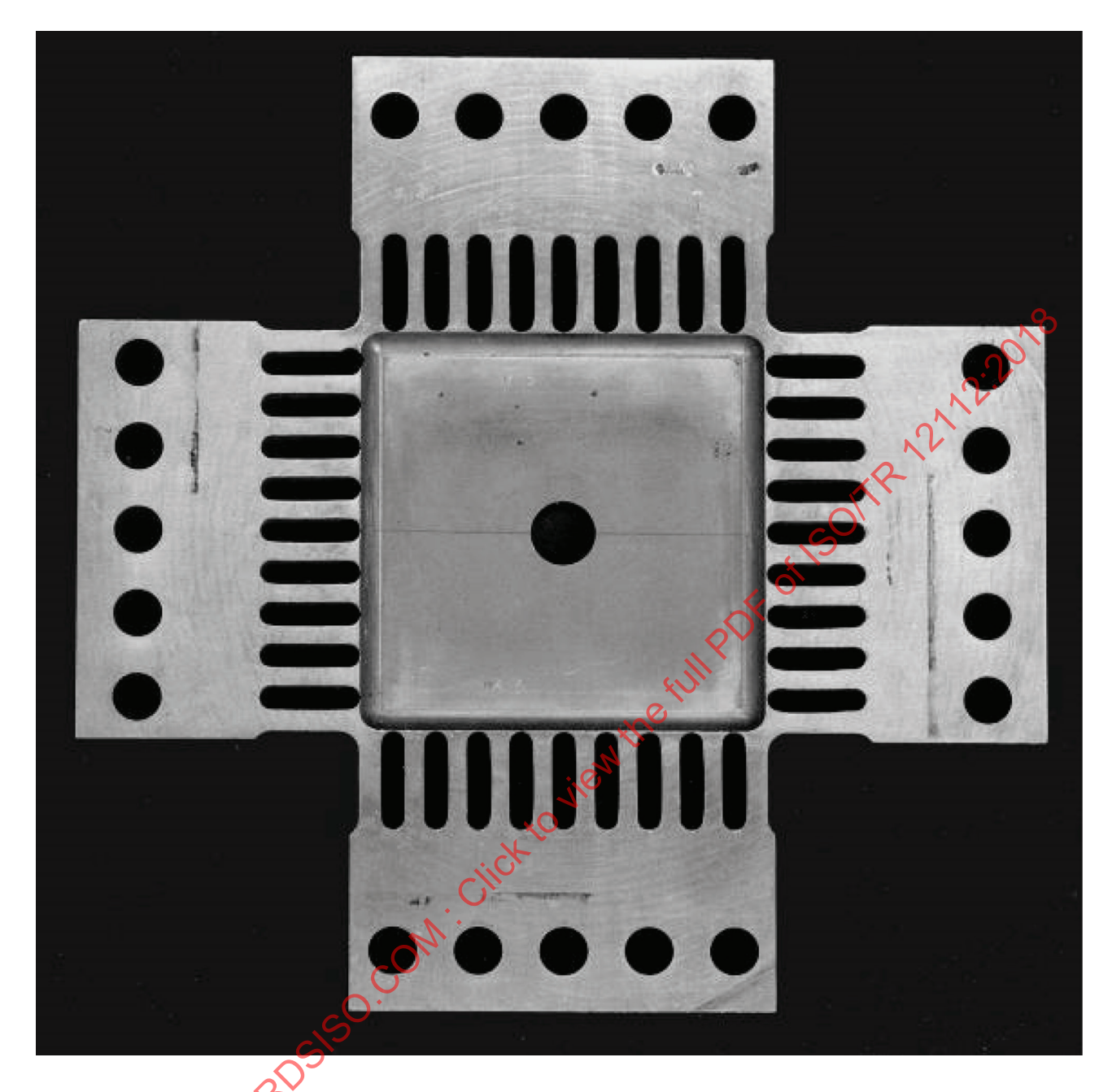


Figure 4 — Sheffield cruciform specimen

6.3 Machine design

6.3.1 Frame

An annular frame with four servo-hydraulic actuators is typical for all cruciform applications. Inplane stiffness should be maximized to minimize frame deflections. Out-of-plane stiffness should be maximized to minimize buckling.

Alignment should be to ISO 23788 for each axis and a mutual orthogonality of $\pm 0.05^{\circ}$ should be ensured.

6.3.2 Loadcells

Axial force cells are needed for each actuator. Force rating, stiffness and accuracy class 1 to ISO 7500-1 should be addressed in their specification.

6.3.3 Strain measurement

Extensometers are not easy to design for cruciform specimens. They should be classified in accordance with ISO 9513 if supplied. Strain gauges may be applied; however, zero drift with increasing LCF cycles is an issue. A reported research technique^[21] is to use strain gauges to establish force or position limits on the two axes, then cycle to failure in force or position control.

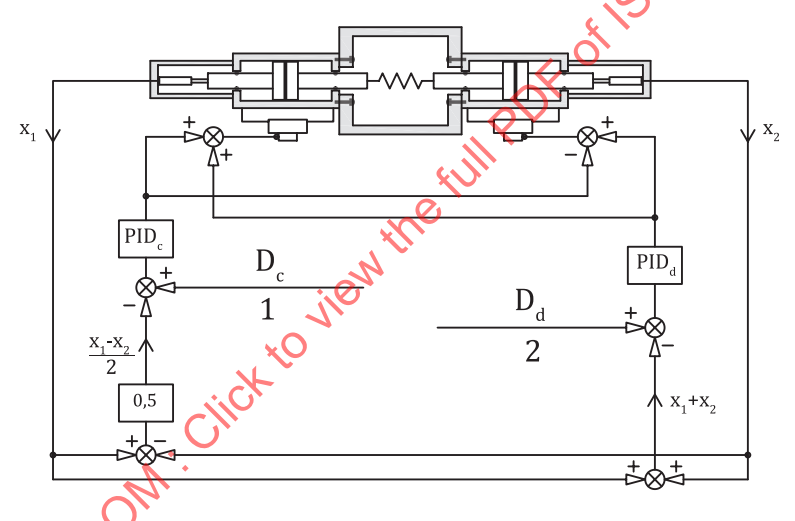
6.3.4 Crack growth monitoring

Non-contact methods such as long focal length (confocal) microscopy are recommended.

6.3.5 Control

Closed loop control should permit bumpless starts and mode transfers between position and force control modes. The control bandwidth should be high enough to accommodate the highest frequency components within the anticipated demand waveforms. Synchronisation of applied waveforms should be better than 0,2°.

Control of centre position, which is a key aspect for cruciform[23] (see Figure 5) should be specified at ±2,5 microns.



Key

- 1 Centre position demand (D_c) = Half-difference of LVDT readings
 - or for zero side force = Difference of Loadcell readings
- 2 Deformation demand (D_d) = Sum of LVDT readings, or
 - = Average of loadcell readings, or
 - = Extensometer reading

Figure 5 — Control of centre position and deformation - one axis of cruciform rig

6.3.6 Data acquisition

Sampling rate should be sufficiently high to avoid aliasing at the highest anticipated frequency components of measured signals. Data skew between measured signals should be less than $5 \mu s$.

6.3.7 Software

Results of data analysis should permit independent verification.

7 Axial + differential pressure systems and specimen design

7.1 Historical development

The combination of cyclic axial force + differential pressure, acting in-phase or in anti-phase, on a thin walled tubular specimen enables the full range of surface biaxiality to be achieved in principle.

In the late 1960s, the application of cyclic axial force + repeated internal pressure on thin walled aluminium alloy tubes was reported. Absence of external pressure to fully reverse the stress cycle means that hardening and ratchetting takes place and cycles became elastic. Nevertheless this system has been used extensively from the 1970s onwards, latterly with added torsion, especially in Germany in support of the automotive industry.

At the University of Waterloo, a system was developed in which axial force was coupled to internal or external pressure, enabling cycle reversal. However, since the pressure was derived from the axial actuator hydraulics, the specimen design had to be changed to alter the biaxial stress ratio [24].

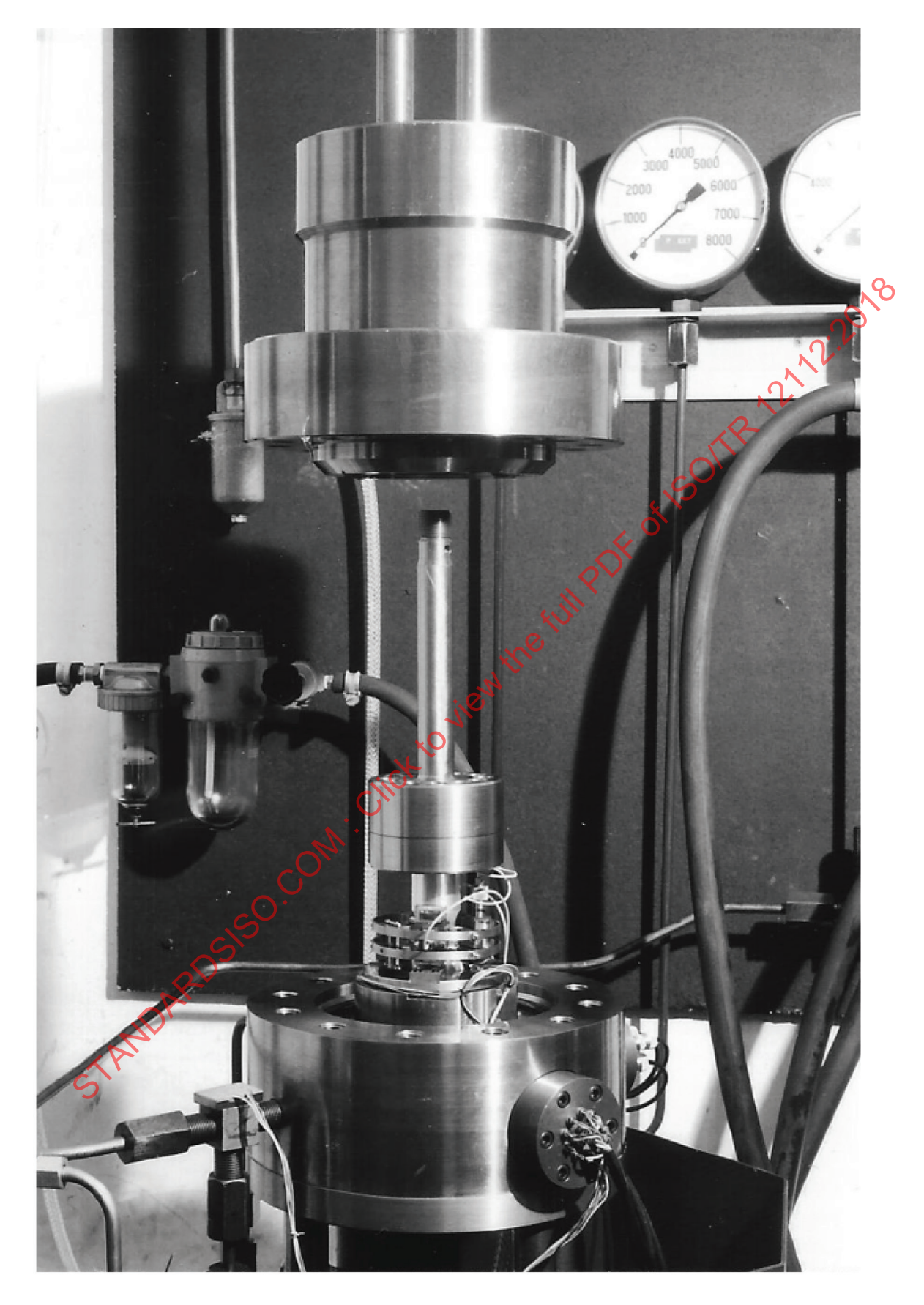
At Bristol University in the 1970s, dual closed loop servo hydraulic systems were used to independently control axial force and differential pressure. The development of extensometry permitted axial and hoop strain to be measured and hysteresis loops generated for both axes[25]. See Figures 6 and 7.

At Sheffield University, a more complex servo-hydraulic system was successfully developed with four independent control loops for axial force, internal and external pressure and torsion, thereby providing the additional ability to investigate rotation of principal stress axes.

16



 $Figure\ 6 - Bristol\ biaxial\ specimen + diametral\ extensometry$



Figure~7-Bristol~biaxial~loadstring+pressure~vessel

7.2 Specimen design

7.2.1 Design considerations

Thin walled tubular specimens enable a potentially large volume of material to be subjected to a constant state of biaxial surface stress and relatively constant radial stress.

A single specimen geometry should be maintained for a given test series to validate data intercomparison.

Bending will be minimized by ensuring that specimen ends are square to the axis and parallel to each other. It is preferable to locate just one end concentrically, which avoids "S type" bending due to any slight misalignment of the machine grips.

Buckling can occur both elastically and plastically. It is strongly influenced by specimen geometry, i.e. parallel length (l_p) , mean diameter (d_m) and wall thickness (t). In addition, the stress or strain ratio is relevant, e.g. equibiaxial stressing when compressive axial force is coupled with high external pressure at one end of the cycle is particularly challenging. Finally in LCF the plastic strain range amplitude and strain hardening characteristics of the specimen material are likely to limit the maximum strain range attainable before instability causes premature failure.

Fatigue strength and life are enhanced by minimizing the stress concentration at the run-out of the fillet radius (*r*) on to the parallel length.

7.2.2 Design recommendations

By considering the geometric ratios l_p/d_m , r/d_m and d_m/t , it is possible to compare the designs of research specimens over the past 50 years. See Annex A, where data has been separately analysed for HCF and LCF.

It can be observed that the ranges for $d_{\rm m}/t$ substantially overlap, which reflects the need to yield the specimen by differential pressures that are not unreasonably high. The ranges for $r/d_{\rm m}$ partially overlap with lower ratios providing more buckling resistance. However, the ranges for $l_{\rm p}/d_{\rm m}$ are essentially contiguous, this being the principal geometric variable to control buckling.

As a result, the recommended ranges for the non-dimensional geometric ratios are:

$$1.5 > l_p/d_m > 0.3$$
 $2.0 > r/d_m > 0.5$ $45 > d_m/t > 15$

Low ratios are indicated for highest plastic strain amplitudes (LCF) and lowest strain hardening rates, whereas high ratios confer the best elastic strain uniformity (HCF). The final design is a compromise between minimum stress concentration and maximum resistance to buckling.

Figure 8 below indicates an LCF specimen design with mid value geometric ratio for d_m/t , a low to mid value for r/d_m and a low value for l_p/d_m .

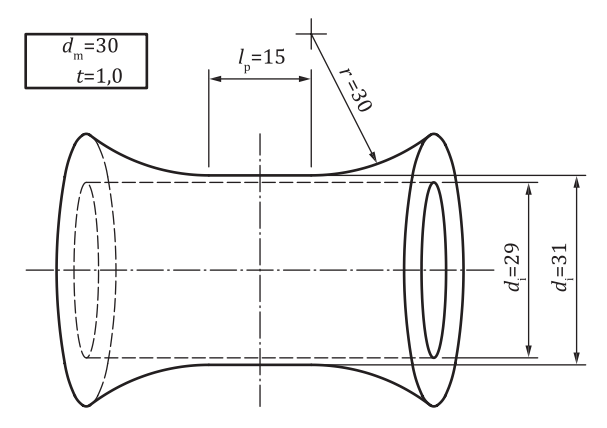


Figure 8 — Axial + internal pressure LCF fatigue specimen

7.2.3 Axial stress due to pressure

The effect of internal pressure on a thin walled tube is to introduce a hoop stress of $Pd_m/2t$. If the tube is closed at one end, the axial stress = $Pd_m/4t$, leading to a biaxial stress ratio (ψ) of 0,5.

If an internal mandrel is fitted, with hydraulic seals at either end acting on the internal diameter, the axial stress is eliminated. However, some hysteresis is introduced axially due to seal friction.

7.3 Machine design

7.3.1 Frame

Axial stiffness should be maximized to minimize frame deflections. Lateral stiffness should be maximized to minimize axial buckling tendency. Alignment should be to ISO 23788.

7.3.2 Pressure containment

Every effort should be made to minimize the free volume of pressurizing oil by fitting a plug/mandrel within the specimen and keeping an external vessel as compact as possible. A safety valve should be fitted in case of control malfunction. These recommendations are safety critical.

In the case of gas pressurization for elevated temperature testing, stored energies can be so great that location of the test machine in a bunker with remote operation is strongly recommended.

7.3.3 Differential pressure

If external pressure is fixed at an intermediate level, internal pressure may be cycled above and below it to create cyclic differential pressure. This approach can be realized with a simple pump and regulator for external pressure and a servo controlled actuator intensifier to modulate the internal pressure with control feedback from a pressure transducer or diametral extensometry.

7.3.4 Force measurement

The axial loadcell should be in accordance with ISO 7500-1. Class 1.

7.3.5 Pressure measurement

The differential pressure sensor (or pair of pressure sensors for internal and external pressure) should meet accuracy conditions similar to the loadcell.

7.3.6 Strain measurement

Extensometry, axial and diametral, should be in accordance with ISO 9513, Class 0,5. Operating force, clamping force and compatibility with environmental chambers and furnaces should also be considered.

7.3.7 Control

Closed loop control should permit bumpless starts and mode transfers between position, force or pressure, and strain control modes. The control bandwidth should be high enough to accommodate the highest frequency components within the anticipated demand waveforms. Synchronisation of applied waveforms should be better than 0.2° .

7.3.8 Data acquisition

Sampling rate should be sufficiently high to avoid aliasing at the highest anticipated frequency components of measured signals. Data skew between measured signals should be less than $5 \,\mu s$.

7.3.9 Software

Results of data analysis should permit independent verification.

STANDARDS ISO COM. Click to view the full Patr of ISO TR. 12.112.2018

Annex A

Historical analysis of specimen geometry

This annex provides an analysis of tubular specimen geometries used in multiaxial research spanning 50 years up to circa 2010, specifically addressing axial + torsion testing and axial + differential pressure testing under LCF and HCF conditions.

A prerequisite for inclusion in the analysis was specimen dimensional information for parallel length, gauge mean diameter, gauge wall thickness and fillet radius at the ends of the parallel length.

The specimen geometric ratios $l_{\rm p}/d_{\rm m}$, $r/d_{\rm m}$ and $d_{\rm m}/t$ are judged to be the most significant in specimen behaviour and their determination is the basis of the analysis. By omitting the highest and lowest values within each set of ratios, recommended ranges are suggested. However, Figures A1 and A.2 include all the data.

A total of 45 specimen geometries (#) have been analysed, as shown in <u>Tables A.1</u> to <u>A.4</u>. Column 1 is headed # in each Table and the references are listed in the Bibliography. In the two Figures, the # references are shown along the horizontal axis of each graph, with the publication dates trending from the oldest on the left to the most recent on the right.

There are four occasions where two # references link to a single author reference. In another four cases, two author references link to a single # reference.

For axial + torsion, LCF, the geometric recommendations within ASTM E2207 have been converted to the same ratios for comparison purposes.

This information is aimed at facilitating the selection of suitable specimen gauge length geometries in future multiaxial research programs.

Table A.1 — Tubular specimen statistics, axial + torsion, LCF

#	Author/Institute	Date	<i>l</i> p	r	d_0	di	d _m	t	l _p /d _m	r/d _m	d _m /t
1	Yokobori et al./ Tohoku ^[16]	1965	25,00	15,00	14,00	11,00	12,50	1,50	2,00	1,20	8,33
2	Liddle and Mill- er/ Cambridge[26]	1973	25,40	22,00	19,00	16,00	17,50	1,50	1,45	1,26	11,67
3	Kanazawa et al./ Cambridge ^[27]	1977	25,40	24,50	22,20	15,90	19,05	3,15	1,33	1,29	6,05
4	Hamada et al./ Ritsumeikan ^[28]	1984	15,00	5,00	12,00	9,00	10,50	1,50	1,43	0,48	7,00
5	Fash et al./ Univ. Illinois[29]	1985	33,00	86,00	29,10	25,00	27,05	2,05	1,22	3,18	13,20
6	Kuwabara et al./ CRIEPI[30]	1987	20,00	20,00	13,00	10,00	11,50	1,50	1,74	1,74	7,67
7	Hug, Esderts/ TU Clausthal[31] [32]	1994/5	40,00	60,00	22,00	19,00	20,50	1,50	1,95	2,93	13,67
8	Ziebs et al./ BAM, Berlin[33]	1995	50,00	39,00	26,50	24,00	2 5,2 5	1,25	1,98	1,54	20,20
9	Kalluri and Bonacuse/ NASA Lewis[19]	1997	41,00	86,00	26,00	22,00	24,00	2,00	1,71	3,58	12,00
10	Calloch and Marquis/ Cachan[34]	1997	30,00	100,0	25,40	22,34	23,87	1,53	1,26	4,19	15,60
11	Lissenden et al./ Penn. State[35]	2000	40,60	86,10	26,00	22,00	24,00	2,00	1,69	3,59	12,00
12	Zamrik and Renauld/ Penn. State[36]	2000	31,75	19,05	12,70	9,70	11,20	1,50	2,83	1,70	7,47
13	Brookes SP et al./ BAM, Berlin[37]	2010	28,00	22,00	12,00	10,00	11,00	1,00	2,55	2,00	11,00
	Arithmetic avera	ges							1,78	2,21	11,22
	Range excl. high	ind low v	alues						1,2- 2,6	1,2- 3,6	7,0- 16,0
	ASTM E2207 - 08 (2013)e1	2008									
	Nominal value		1,5 d _o	$3,2 d_o$	14 t	0,85 d _o		2 typi- cal			
	± semi-range		0,5 d _o	0,4 d ₀	3 t	0,04 d ₀		0,5			
	Mean values for t = 2 mm		42	89,6	28	23,8	25,9	2	1,62	3,46	12,95

Key

 l_p = parallel length

r = blend radius

 d_0 = outside diameter

 d_i = inside diameter

 $d_{\rm m}$ = mean diameter

t = wall thickness

Table A.2 — Tubular specimen statistics, axial + torsion, HCF

#	Author/Institute	Date	l_{p}	r	d_0	$d_{\rm i}$	d _m	t	$l_{\rm p}/d_{\rm m}$	r/d _m	d _m /t
14	Blatherwick and Viste/Minneso- ta[38]	1967	44,50	19,00	23,57	22,30	22,94	0,64	1,94	0,83	36,12
15	Baier/ TU Stuttgart[39]	1970	15,00	40,00	21,00	17,00	19,00	2,00	0,79	2,11	9,50
16	Lempp/ TU Stuttgart[40]	1977	70,00	75,00	69,00	65,00	67,00	2,00	1,04	1,12	33,50
17	ibid[<u>40</u>]		70,00	75,00	68,00	65,00	66,50	1,50	1,05	1,13	44,33
18	Rode, Bolz/ TU Braun- schweig[41] [42]	1987/ 94	40,00	62,50	29,00	26,00	27,50	1,50	1,45	2,27	18,33
19	El-Magd et al./ RWTH Aachen [43]	1977	50,00	80,00	21,20	20,00	20,60	0,60	2,43	3,88	34,33
20	Kaniut/ RWTH Aachen[44]	1983	40,00	40,00	34,00	32,00	33,00	1,00	1,21	1,21	33,00
21	Brune/ TU Clausthal ^[45]	1991	60,00	30,00	34,00	31,00	32,50	1,50	1,85	0,92	21,67
22	ibid[45]		60,00	30,00	35,00	32,00	33,50	1,50	1,79	0,90	22,33
23	Löwisch et al./ TU Bremen[46]	2000	30,00	50,00	21,00	18,00	19,50	1,50	1,54	2,56	13,00
	Arithmetic averag	ges				9	in.		1,51	1,69	26,61
	Range excl. high a	nd low v	alues			SWILLE			1,0- 2,5	0,9- 3,0	13- 36,0
Key					is is	S					
$l_{\rm p} = {\rm pa}$	arallel length				×O						
r = ble	end radius				<i>Y</i>						
$d_0 = 0$	utside diameter										
$d_{\rm i} = {\rm ir}$	iside diameter			.							
$d_{\rm m} = 1$	mean diameter		-0	7,							
t = wa	all thickness		\mathcal{C}								
		.6	9 .								
		S									
	STANDARDSISO.										
	CXY										
- 9											

Key

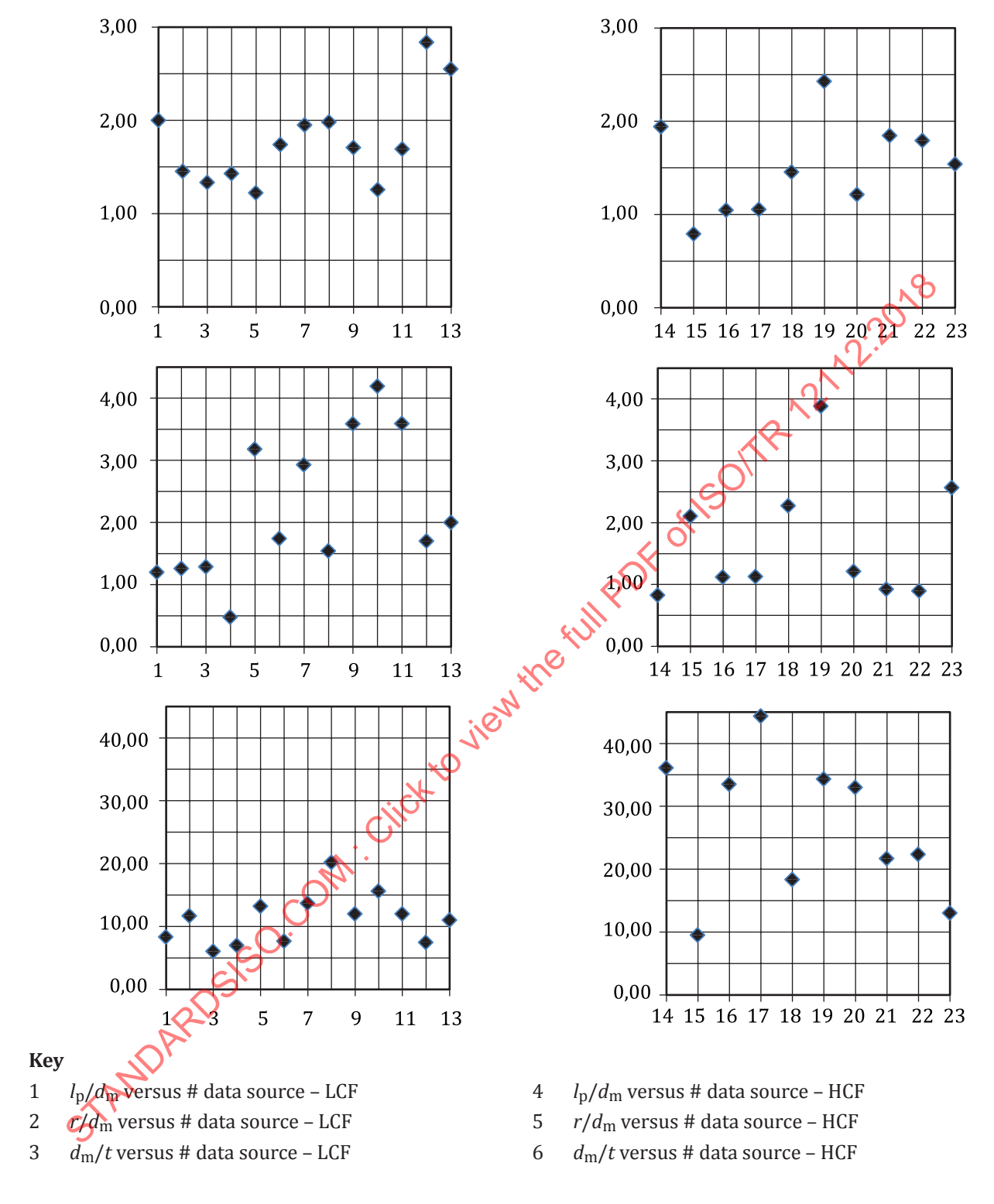


Figure A.1 — Specimen geometry ratios for axial + torsion, LCF and HCF

Table A.3 — Tubular specimen statistics, axial + differential pressure, LCF

#	Author/Institute	Date	l_{p}	r	d_0	di	d _m	t	$l_{\rm p}/d_{\rm m}$	r/d _m	d _m /t
24	Kennedy/ ORNL[<u>47</u>]	1963	25,40	3,20	24,40	21,40	22,90	1,50	1,11	0,14	15,27
25	Havard and Topper/Water- loo[²⁴]	1969	6,35	25,40	32,75	31,75	32,25	0,50	0,20	0,79	64,50
26	ibid[24]		6,35	25,40	59,39	57,15	58,27	1,12	0,11	0,44	52,03
27	Andrews and Ellison/Bristol ^[9]	1973	15,90	12,70	27,44	25,40	26,42	1,02	0,60	0,48	25,90
28	Lohr and Ellison/ Bristol[25]	1980	9,50	25,40	26,98	25,40	26,19	0,79	0,36	0,97	33,15
29	Found et al./ Sheffield ^[10]	1985	20,00	25,00	22,30	18,00	20,15	2,15	0,99	1,24	9,37
30	Shatil et al./ Bristol ^[48]	1994	9,50	25,40	27,44	25,40	26,42	1,02	0,36	0,96	25,90
31	Varvani and Top- per/Waterloo[49]	1999	0,00	36,00	59,00	57,00	58,00	1,00	0,00	0,62	58,00
32	Weick et al./ TU Karlsruhe[50]	2001	25,00	100,0	55,70	53,70	54,70	1,00	0,46	1,83	54,70
	Arithmetic averages Range excl. high and low values parallel length lend radius putside diameter mean diameter mean diameter all thickness								0,47	0,83	37,65
	Range excl. high a	nd low	values			\$	illi,		0,1- 1,0	0,4- 1,3	15- 58,0
Key						ille					
l * -	arallel length				. (N					
	end radius				j'						
	utside diameter				140						
$d_{\rm i} = {\rm in}$	iside diameter			111	3/-						
$d_{\rm m} = r$	nean diameter			'C''							
t = wa	all thickness			<i>.</i>							
t = wall thickness STANDARDSISO.											

Key